Characterization of deformation twinning in polycrystalline cobalt A quantitative analysis

M. Martinez, E. Hug

Characterization of deformation twinning in polycrystalline cobalt:

a quantitative analysis

Mayerling Martinez[1*], Eric Hug[1]

[1] Laboratoire de Cristallographie et Sciences des Matériaux, Normandie Université, CNRS UMR 6508, 6 Boulevard Maréchal Juin, 14050 Caen, France

* corresponding author: mayerling.martinez@ensicaen.fr

Abstract

Electron backscattering diffraction technique was used for a statistical analysis of twin formation in deformed polycrystalline cobalt. Deformation microstructure of samples plastically strained after a monotonous tensile test was studied by scanning and transmission electron microscopy. The analysis shows that the principal twin mode is the tension $\{10\bar{1}2\}$ type. Multiple twin variants of this mode are present inside a grain. The higher occurrence corresponds to the variant with the misorientation of about 60° giving the best strain accommodation. It was found that besides grains favorably oriented, which are more prone to twin, there is also twinning in some grains not favorably oriented, which points out an influence of the local state of internal stress. Grain orientation has a more pronounced impact on twinning characteristics than the grain size. Favorably oriented grains exhibit a strong and positive correlation of the twin frequency, the twin area fraction, and the presence of multi-variant twins in a grain. On the other hand, large grains are more prone to twin, exhibit several twin variants but small twin area fraction.

Key words: polycrystalline cobalt, twinning, hcp metal, grain size, grain orientation.

1. Introduction

Deformation twinning represents an important deformation mode in polycrystalline hexagonal close packed (*hcp*) metals. There are multiple twin systems in hexagonal metals and hence it is expected that different twin types could operate conditioning on loading conditions and the *c*/*a* ratio [1]. Depending on the crystal parameters of the hexagonal structure, a given twin system may induce either a dilatation or a contraction along the *c*-axis, which are called tension or compression twins, respectively. The most commonly activated system in *hcp* metals is the $\{10\bar{1}2\}$ type, because the corresponding twinning shear magnitude is the lowest. For cobalt, with a ratio $c/a < \sqrt{3}$, this corresponds to a tension twin, which is expected to be activated when tensile stress is applied parallel to the *c*-axis. Besides the $\{10\bar{1}2\}$ type, others twin modes have been observed in hexagonal metals: $\{11\bar{2}1\}$ and $\{11\bar{2}2\}$ twins in titanium and zirconium [2-5], $\{10\bar{1}1\}$ and $\{10\bar{1}3\}$ types in magnesium [6], and $\{10\bar{1}1\}, \{10\bar{1}3\}$ and $\{11\bar{2}1\}$ types in cobalt [7,8].

In order to have a wider understanding of twinning in hexagonal metals, efforts have been made recently to provide statistical analysis of the occurrence of twinning under various conditions of load, using an automated electron backscattering diffraction (EBSD) technique. Beyerlein et al. [9] focused on the study of $\{10\bar{1}2\}$ twins in high purity Mg. The samples were deformed in a compression test up to 3% strain and the relationships between

orientation of grains, grain size, thickness and numbers of twins were established. Capolungo et al. [10] published a similar study for the $\{10\bar{1}2\}$ twins in Zr. Samples of polycrystalline Zr were loaded in compression to 5% and 10% strain in this study. More recently, Kumar et al. (2018) published a study concerning Ti, the samples were also deformed in a compression test and the study was extended to several types of twins, namely $\{10\bar{1}2\}$, $\{11\bar{2}1\}$, and $\{11\bar{2}2\}$. The $\{10\bar{1}2\}$ twinning is possible on six equivalent $\{10\bar{1}2\}$ twinning planes with a specific shear direction of the $\langle 10\bar{1}1\rangle$ type. The mechanism of activation of specific twin variants in Mg and Mg alloys has been studied by several authors [11-13].

Two reports concerning a statistical analysis of twinning in polycrystalline Co have been published so far. Zhang et al.[7] performed a statistical analysis, based on EBSD, of the frequency of different types of twins for samples after compression and dynamic plastic deformation test. The second study, by Martinez et al. [8], presents an analysis using identification of twins by transmission electron microscopy (TEM) after a monotonous tensile test. These two studies led to the conclusion that the most important twin mode, regardless the deformation mode, is the $\{10\bar{1}2\}$ type. Others studies dealing with twinning in Co were rather focused on high resolution transmission electron microscopy studies of twin/matrix interfaces of different types of twins [14-16].

The aim of the present study is to reach a better understanding of the twinning process in *hcp* cobalt. The use of the electron backscattered diffraction technique in strained polycrystalline cobalt allowed acquiring an important quantity of data, thus allowing a statistical analysis considering aspects such as grain orientation, twin volume fraction,

twinning modes and twin variants. These are interesting aspects recently explored for other hexagonal metals, but not yet for polycrystalline cobalt. The objective in the present work is to present a statistical analysis of the features based on a grain by grain investigation of the twinning in a large number of grains.

2. Material and Experimental details

Rolled sheets of polycrystalline cobalt (99.9 wt. % purity) were selected to study deformation twinning. The as-received material was annealed under secondary vacuum at 1100 °C for 1 h. The characterization of the initial state was performed in the previous study by EBSD [8, 17]. The analysis of initial material shows that the samples contain about 8.5% of residual *fcc* cobalt (Figure 1a). The results indicated (Figure 1b) the typical basal {0001} texture of hexagonal rolled metals [18], with basal poles tilted ±30-50° away from the normal direction [8]. The mean grain size is around 19 µm (~295 μm^2).

The microstructure of samples plastically strained at a value of 0.04 was studied by EBSD coupled to a Scanning Electron Microscope (SEM). Three distinct stages are present on the work-hardening curve of polycrystalline cobalt: a nonlinear elasticity stage, a second one linked to basal slip mechanisms, and a last one associated to the mechanical twinning generalization. The chosen strain level (4%) corresponds to the work hardening stage during which twinning is the predominant deformation mechanism [8]. Interrupted tensile tests were performed parallel to the rolling direction (RD) of the sheet at the strain rate of

$2 \times 10^{-4}\ s^{-1}$. The samples were dog bone shaped with a gauge section of 20 mm in length and 10 mm in width. Strain was measured by a traditional clip-on extensometer.

The samples for EBSD analysis were prepared by mechanical grinding until 1 µm diamond paste, followed by a final electrolytic polishing using a solution of glycerol, perchloric acid and ethanol at a voltage of 20 V. The EBSD data were obtained using the ZEISS Supra 55 system operating at 20 kV with a 0.2 µm step size. The microscope was equipped with the TSL/EDAX data acquisition software and the CDD camera DigiView 3. The data were collected from different scans covering the total surface area around 0.5 mm^2, allowing the analysis of 500 grains.

The fraction of twinned grains was measured, one twinned grain being considered as a grain that contains at least one visible twin. The extent of twin formation regarding the grain orientation and the grain size area was determined. The grain size orientation is defined in the present work as the misorientation angle between the *c*-axis of the grain and the direction of the macroscopic stress applied to the samples. The calculation of the area of the grain includes any twinned regions. The twin area fraction was determined, as well. Grain area and twin area data are based on 2D analysis of the material. For each twinned grain the number of variants was also determined. Table 1 shows the shear stress associated to some twin mode and other crystallographic parameters.

Table 1. Twins characteristics of some twins in cobalt [7].

Twin plane	Rotation		Magnitude of the twinning shear	Twin type
	Angle	Axis		
$\{10\bar{1}2\}$	86°	$\langle 1\bar{2}10\rangle$	0.13	Tension
$\{11\bar{2}1\}$	34°	$\langle 1\bar{2}10\rangle$	0.62	Tension
$\{10\bar{1}1\}$	56°	$\langle 1\bar{2}10\rangle$	0.14	Compression
$\{10\bar{1}3\}$	64°	$\langle 1\bar{2}10\rangle$	0.35	Compression

Samples were also examined by TEM. Conventional bright field images were made with a Jeol 2010 TEM operating at 200 kV. Samples for TEM observations were prepared by mechanical polishing and then electropolished by the twin jet method in a Struers Tenupol5, with an electrolyte consisting of 90% glacial acetic acid and of 10% perchloric acid at a voltage of 50 V.

3. Results and Discussion

3.1 Microstructure and twin variant analysis

The present analysis concerns the study of deformation twinning on samples plastically strained in the twinning work hardening stage and the description of morphology and types of twin variants. Figure 1 represents the pole figure and a general view of the strained sample obtained by EBSD analysis. The grayscale (Figure 1d) represents the quality of the Kikuchi pattern. Twins are also represented in two colors and one can readily see that a high proportion of grains are twinned. The most common twin encountered are tension twins, the $\{10\bar{1}2\}$ type that is represented in red, and the $\{11\bar{2}1\}$ type represented in blue. Twins exhibit variable sizes, some of them occupying the whole grain and others ending

inside the grain. Twins of a $\{10\bar{1}2\}$ type have lenticular or irregular shapes while the twins of $\{11\bar{2}1\}$ type are very long and feature extremely flat interfaces. In some grains different variants of the same type of twin are present. In others cases, the two types of twins with their different variants can be observed. No twins appear to cross grain boundaries, or to be connected to each other at grain boundaries, as it was previously observed for Mg and Mg alloys [9,19]. Double twinning and others twin modes have already been observed in cobalt [7,8], however, there is no evidence of these twin modes in our samples, using the EBSD experimental conditions with the step size of 0.2 µm. TEM is a more suitable technique to reveal the presence of small single twins or double twins, as show at the end of this section. According to the histogram of grain area in Figure 1e, grain surface area is principally in a range reaching about 650 μm^2.

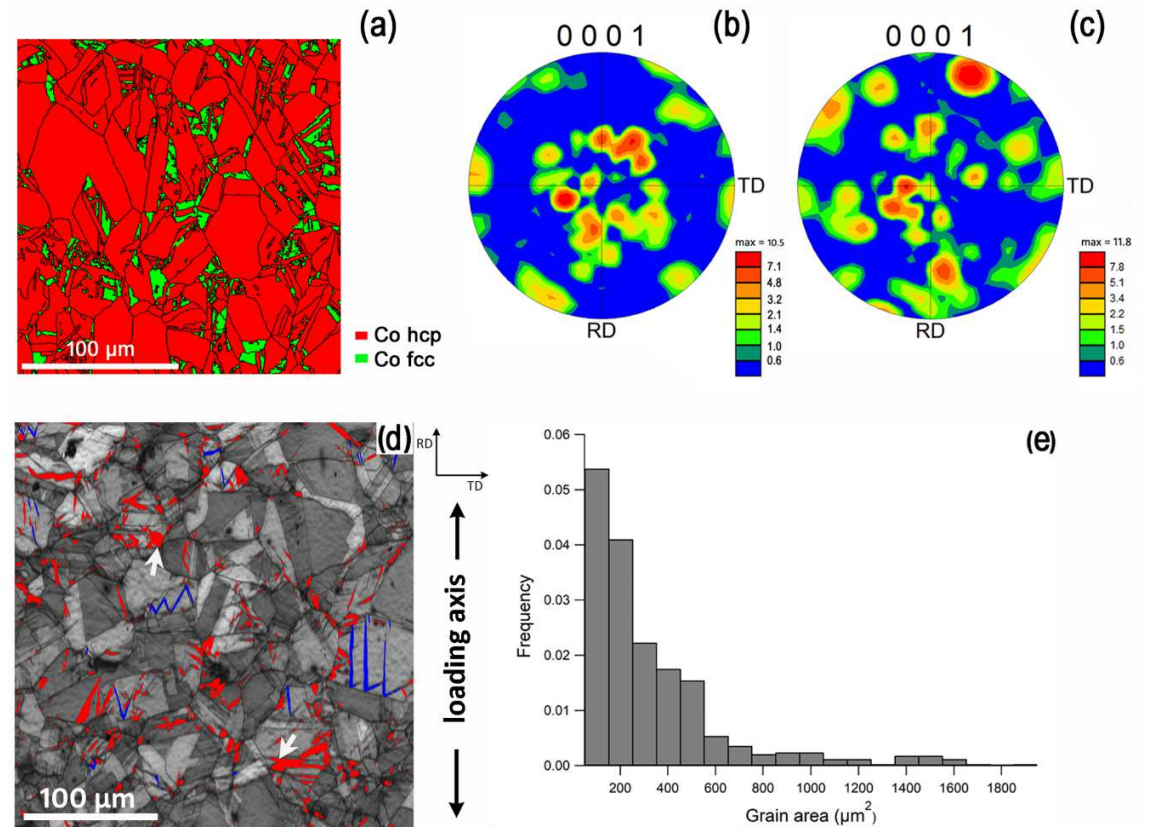

Figure 1. Microstructure of polycrystalline cobalt: (a) distribution of phases after annealing (grain boundaries are shown in black); (b) pole figure showing texture component after annealing, (c) pole figure after straining at 4%; (d) representation of the Image Quality maps after straining at 4%, the grey scale represents the quality of the Kikuchi pattern from high (white) to low (black). Tension $\{10\bar{1}2\}$ twins are represented in red and $\{11\bar{2}1\}$ in blue; (e) grain area distribution of polycrystalline samples.

One example of a grain with its *c*-axis almost parallel to the loading axis within ≈ 5° is presented in Figure 2. The grain exhibits two types of twins and different variants for each twin type. Figure 2a represents the inverse pole figure of the region and for the sake of

simplicity a different color code is used in Figure 2b which is consistent with the colors as present in pole figures (Figure 2c).

The twins with lenticular or irregular shapes, labeled as T1a and T1b, correspond to different variants of $\{10\bar{1}2\}$ twin mode. It is clear from the pole figure that $\langle 1\bar{2}10\rangle$ is a common axis between the matrix (M) and T1a and M and T1b (only the relation of M and T1a is indicated in Figure 2c, red circle). Each twin is rotated 86° away from the $\langle 1\bar{2}10\rangle$ axis of the matrix; it can be seen that the rotation axis is the same for both twins and that the twin to twin misorientation is about 10° as indicated in the $\{0001\}$ pole figure.

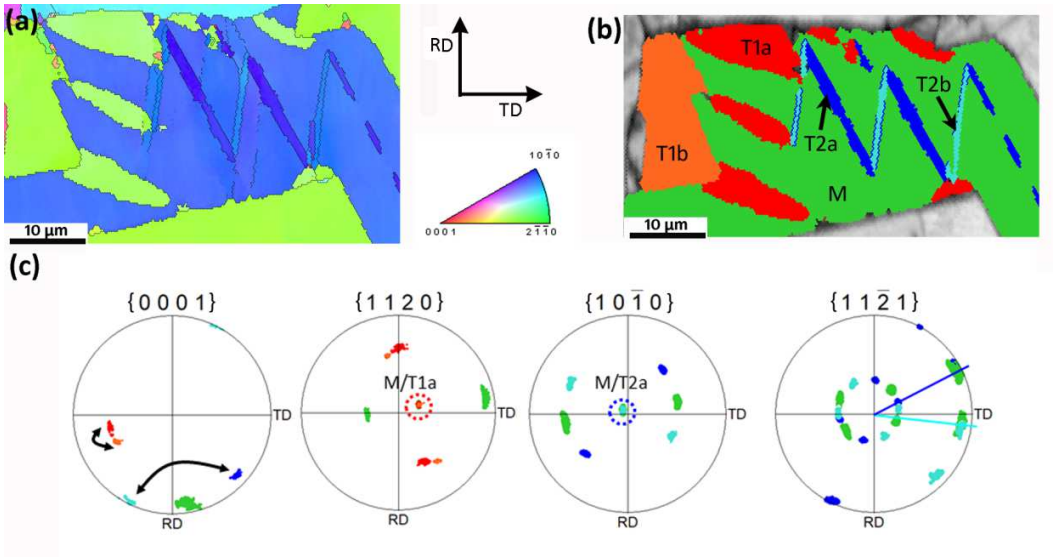

Figure 2. Image of a grain with its *c*-axis nearly parallel to the direction RD of the macroscopic stress. The EBSD map shows the co-existence of several types of twins: (a) inverse pole figure map of the grain, (b) image showing the color code associated to (c) pole figure showing the crystallographic relationship between the matrix and the twins.

Theoretically, the $\{10\bar{1}2\}$ twinning is possible on six equivalent $\{10\bar{1}2\}$ twinning planes with a specific shear direction of $\langle 10\bar{1}1\rangle$ (six equivalent twin variants, or three twin variant pairs). The disorientation relationship between identical variants is 0°, between twins of the same variant around 7° and for twins of different variants about 60° [13,20,21]. Consequently, according to the misorientation between T1a and T1b, we can conclude that these twins constitute a variant pair. The difference in the misorientation relationship is certainly due to the orientation spread induced by the slip activity. Regarding the frequency, in one third of the cases where several twins were encountered inside a grain, the $\{10\bar{1}2\}$ variant pairs were identified.

One can also observe two others twin types (labelled T2a and T2b), which exhibit extremely flat interfaces and correspond to the $\{11\bar{2}1\}$ mode. According to the color code and the pole figure, $\langle 10\bar{1}0\rangle$ clearly appears to be a common axis to M and T2a and to M and T2b (only the relation of M and T2a is indicated in the Figure 2c, blue circle). The twins are rotated away from the axis at 34° around the same $\langle 10\bar{1}0\rangle$ axis. For this twin type we can conclude that a twin/twin misorientation of about 68° corresponds to a misorientation of a variant pair for the $\{11\bar{2}1\}$ twins, which is very near to the theoretical value of 68.4°, calculated according to the relationship between the twinning shear and the lattice parameters [1]. These twins are always present together with at least one $\{10\bar{1}2\}$ twin variant.

The coherency can be also evaluated using the pole figures of the planes. The traces of the T2a and T2b twin boundary planes are shown on the $\{11\bar{2}1\}$ pole figure (Figure 2c). Each trace is aligned along one normal of the $\{11\bar{2}1\}$ planes indicating their coherency. The analysis of coherency for $\{10\bar{1}2\}$ twins using pole figures is more difficult because of their irregular shape. In addition it is known that $\{10\bar{1}2\}$ twins are not always coherent in cobalt [16,22]. The deviations for the habit planes of $\{10\bar{1}2\}$ twins have been also observed in magnesium [14], some hypothesis have been proposed but there is no consensus regarding these deviations [16,22].

It has to be stressed here that the twin morphology in cobalt is much more irregular than that observed for magnesium, titanium or zirconium. According to observations in, twins observed in Mg alloys, Zr and Ti are rather lenticular shape, and for larger grains the presence of multiple parallel twins is facilitated.

The flat interfaces of the $\{11\bar{2}1\}$ twin are certainly a consequence of its high twinning shear in comparison to that of the $\{10\bar{1}2\}$ mode (Table 1). It was observed that the $\{11\bar{2}1\}$ twins are present in general in large grains with a grain area over 1000 μm^2 in the half of the cases where these twins were encountered. Also, when a variant pair is present inside a grain they are systematically connected to each other.

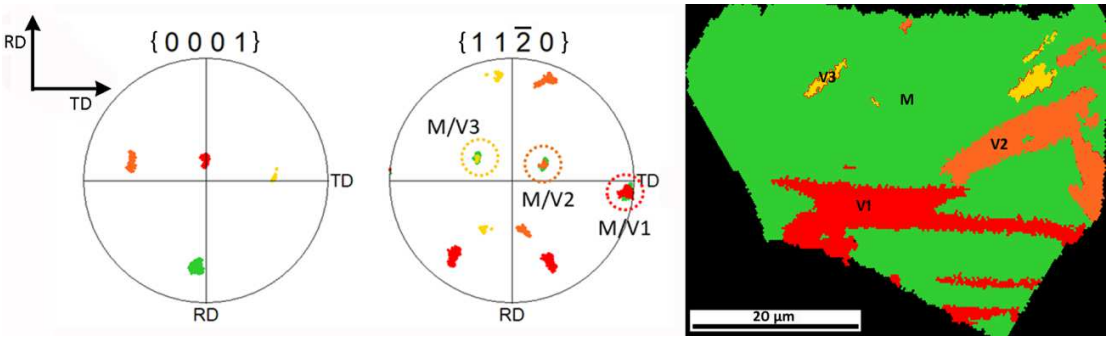

Figure 3. Image of a grain showing the co-existence of several variants of the same type of twin and related inverse pole figures.

Figure 3 shows an example of a grain with multiple variants corresponding to the $\{10\bar{1}2\}$ mode. The matrix (M) is represented in green; each variant is represented in different color and labelled as V1, V2 and V3. Some twins seem to form independently and meet after growth for variants indicated as V1 and V2. The three variants are rotated around the axis type $\langle 1\bar{2}10\rangle$ as seen in the corresponding $\langle 1\bar{2}10\rangle$ pole figure. The three axes (indicated with color circles) are physically different but equivalent from a crystallographic point of view so as they are inclined by 60° from each other. According to this analysis, no variant pairs are present in this grain. In the majority of grains (two-third of cases), when multi-twins were present they correspond to different twin variants, as in the present example.

Guo et al. [12] studied the variant selection using a combined analysis of Schmid factor (m) and local strain accommodation factor (m') during compression of Mg at room temperature. The local strain accommodation refers to the relationship between twinning planes normal and twining shear directions. According to these analyses, twin occurrence is governed not only by the orientation of the grains, but also and mainly by strain

accommodation. For the case of multiple twinning in the same grain, the selection of a variant of higher misorientation (≈ 60°) gives the best strain accommodation, while for a variant pair with misorientation of 7.4° the strain accommodation is the worst. Other studies concerning variants selection of twins in Mg alloys ponder not only the strain and the orientation in the grain, where the twins form or could form, but also the strain accommodation, that is or would be required in neighboring grains [23,24]. The analysis shows that the twin selected depends not only on the value of the Schmid factor. The twin variant selected is the one that requires the least accommodation work in most of the neighboring grains.

Considering these previous studies [12,23,24], the results concerning the variant selection of twin in strained cobalt can be explained as follows. First the higher occurrence of twins (two-third of the cases) with mutual misorientation of 60° is expected, because this corresponds to the best strain accommodation inside the grain. Second, the presence of a still considerable occurrence of variant pairs (in one-third of the cases), could be related to a lowest accommodation work in most of the adjacent grains.

In order to make a complete characterization of twins variants activated during deformation, the samples were also observed using TEM, as depicted in Figures 4 and 5. The $\{10\bar{1}1\}$ and $\{10\bar{1}3\}$ compression twins were observed. The occurrence of these twins was low and their size small, in the order of few hundred nanometers, so as their detection using EBSD could be easily neglected, as in our experiments. The image depicted in Figure 4 shows an example of the $\{10\bar{1}3\}$ compression twin and the diffraction pattern showing the corresponding misorientation. The twin and the matrix are related by a rotation of 64°

about the $\langle 1\bar{2}10\rangle$ axis. The observations revealed a presence of stacking faults in both the matrix and the twin, but their density seems to be higher in the latter case, as revealed by the intensity of streaks in the diffraction pattern.

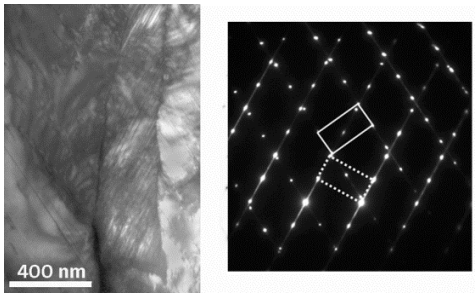

Figure 4. TEM image of the morphology of $\{10\bar{1}3\}$ compression twin and the corresponding diffration pattern. The pattern of the matrix is represented by continous line and for the twin by dotted line.

Two types of double twinning were encountered in these samples, namely the $\{10\bar{1}3\}$-$\{10\bar{1}2\}$ and the $\{10\bar{1}1\}$-$\{10\bar{1}2\}$ modes. An example of the latter case is captured in Figure 5. Double twinning occurs as follows [25]: the basal plane of the matrix first rotates by 56° around the $\langle 1\bar{2}10\rangle$ axis to form the $\{10\bar{1}1\}$ twin, then rotates again around the same axis by 86° to form the second order $\{10\bar{1}2\}$ twin. The final misorientation, between the matrix and the double twinning, is then 38°. The image shows a double-twin, in the process of formation, so that in the diffraction patterns (not showed here) we can measure the three typical misorientations mentioned. More details and descriptions concerning single and double twins can be encountered in [8].

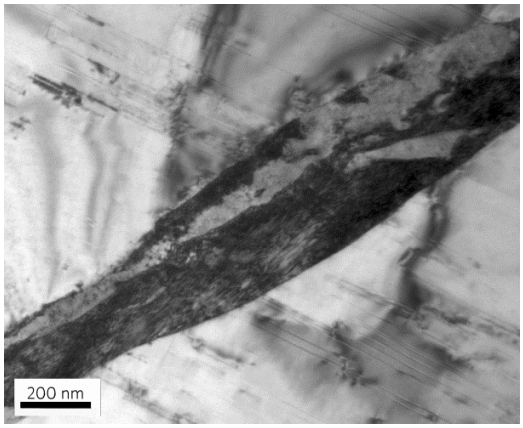

Figure 5. TEM images of the morphology of a $\{10\bar{1}1\}$-$\{10\bar{1}2\}$ double-twin in polycrystalline strained cobalt.

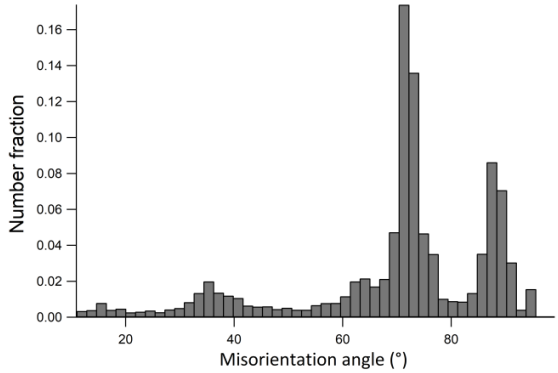

Figure 6. Grain boundary misorientation angle distribution for polycrystalline cobalt strained in misorientation tension to 4%.

The grain misorientation angle distribution obtained by EBSD experiments is shown in Figure 6. The plot axis starts at 10° in order to avoid the intragranular misorientation associated with the presence of dislocations and internal stresses. There are three misorientation angle peaks at around 71°, 86° and 34°, by order of intensity. The peak

located at 71° is associated with the phase transformation during cooling after annealing. Cobalt exhibits a face-centered cubic structure at high temperatures. During cooling the metal transforms into the hexagonal structure at 437 °C. The transformation is martensitic and occurs in the {111} type planes of the *fcc* structure so that this angle can be interpreted as a result of phase transformation following the Shoji-Nishiyama orientation relationship between the *fcc* and *hcp* phases [26]. The two other peaks at around 86° and 34° correspond to the tension twins. They have the same rotation axis $\langle 1\bar{2}10\rangle$, with a rotation of 86° for the $\{10\bar{1}2\}$ twin and 34° for the $\{11\bar{2}1\}$ twin. Plotting of both boundaries (86° and 34°) on orientation maps showed that they are correlated with boundaries having the morphologies consistent with twins [27,28].

3.2 Statistical analysis of twinning

The present section aims at a statistical analysis of twinning in polycrystalline cobalt and a comparison with previous works concerning other hexagonal metals. The analysis was made using 500 grains covering about 0.5 mm^2. For the analysis, the $\{10\bar{1}2\}$ and $\{11\bar{2}1\}$ tension twins and their variants were considered, with special emphasis in the first twin type. The features considered here are the grain area, grain orientation, fraction of twinned grains, twin area fraction, and number of twin variants. The result indicates that 46% of grains are twinned, and that 8% of grains contain two types of tensile twins.

3.2.1. Grain orientation effects on twinning

In order to investigate the orientation effect for each grain, the angle between the *c*-axis and the load axis was determined. This orientation data allow us to determine whether a grain is favorably oriented to deform by generating tensile twins.

Regarding the orientation of grains, it was observed that grains that have their *c*-axis almost parallel to the direction of the applied load are all twinned (Figure 7a), and contain tension twins as expected. However, about 35% of grains are not conveniently oriented for twinning. These grains with their *c*-axis perpendicular to the loading axis also contain tension twins, which is unexpected, since their Schmid factor is in average lower than the values corresponding to grains with their *c*-axi*s* parallel to the loading axis. Tension twins appeared over the whole range of orientations, regardless the orientation of the grains, even for those grains for which the orientation is consistent with a deformation through the formation of compression twins.

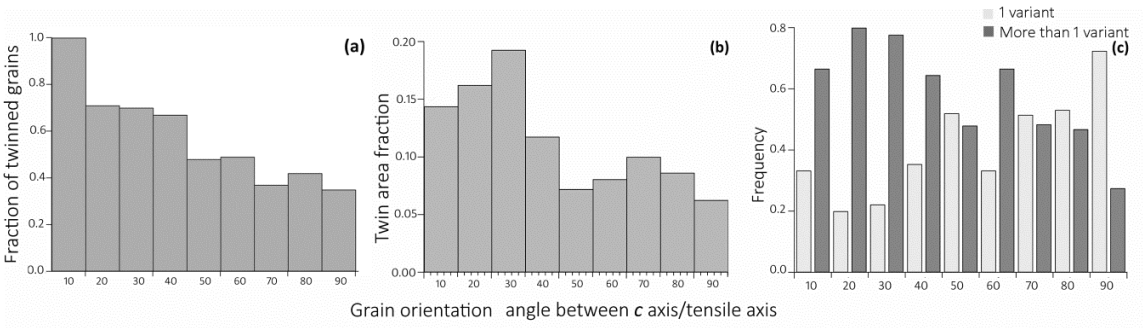

Figure 7. Effects of grain orientation on (a) fraction of twinned grains, (b) twin area fraction and (c) number of variants in the grain.

The influence of grain orientation in the twin area fraction is depicted in Figure 7b. According to our results, there is a decrease in twin area fraction when the grain is less favorably oriented to twinning. The frequency of a grain of a given orientation to twin in one or more variants is captured in Figure 7c. Here we consider that a grain with more than one variant contains different variants of the same twin type, one or several variant pairs, mixtures of different tensile twins, or combinations of two or more of previous cases (Figure 2 and 3). We can observe that grains with their *c*-axis almost parallel to the load axis contain in majority of cases more than one variant, while the grains that are less favorably oriented, with their *c*-axis perpendicular to the macroscopic loading direction, display in most of cases one single variant. Increasing the misorientation angle between the *c*-axis and the loading axis reduces the probability of a grain to exhibit more than one variant.

Our results can be compared with the influence of orientation on the twinning mechanisms of others plastically strained hexagonal metals. The study by Lou et al. [27] concerns the effect of different loading conditions on twinning in magnesium. The samples were subjected to dynamic plastic deformation with the compression axis taken with different angles to the *c*-axis. The observed behavior of Mg is similar to that of Co: the twins are activated in grains during deformation even if the initial orientation does not in theory favor the $\{10\bar{1}2\}$ twinning.

Similar behavior was reported for Mg [9] and Zr [10] in studies using the Schmid factor analysis. A geometric Schmid factor was calculated with respect to the orientation of the

macroscopic loading direction, using the twin plane and the shear direction of each twin variant for each grain. Twinning occur in both types of grains, the favorably oriented with a high Schmid factor (≥ 0.37) and not so favorably oriented, with lower Schmid factor (≤ 0.37). Concerning the specific twins that are formed in grains, the majority of the twins activated are those with a higher Schmid factor, but it is not always the case [9,10].

The presence of twins with low Schmid factor, revealed in the above mentioned studies, and the presence of unexpected high number of twinned grains not favorably oriented, as reported here, can be explained by a deviation in a local grain stress state from a macroscopic stress state, and to local stress fluctuations within the grain, produced by interaction with its neighborhood.

Another parameter evaluated as a function of orientation was the twin area fraction. While Capolungo et al. [10] found for Zr that the twin thickness is insensitive to or only slightly dependent on the grain orientation, Beyerlein et al. [9] reported for Mg that in more favorably oriented grains the twins are thicker (the thickness correspond to the minor axis of an ellipse fitted to each twin). If we extrapolate the thickness to the twin area fraction we can conclude that the behavior of cobalt is similar to that of magnesium, since the twin area fraction increases in more favorable oriented grains.

The influence of grain orientation on the frequency of twinning variants (Fig. 7c) shows that grains favorably oriented for twinning present more twin variants than those unfavorably oriented. The grain orientation effect on the variant selection has been also reported for Zr and Mg [9,10]. These analyses consider the Schmid factor of each twin formed in different grains. It is seen that the favorable variants are those with the higher

Schmid factor, but the number of activated variants in a grain is not clearly evident form these studies, hence no conclusion about this aspect in different *hcp* metals can be drawn.

3.2.2. Grain size area effects on twinning

The influence of the grain size area on various twinning parameters is expressed in the histograms displayed in Figure 8. We decided to include only the grain size area under 650 μm^2 because for larger grains only few cases were present, which do not need to be statistically significant.

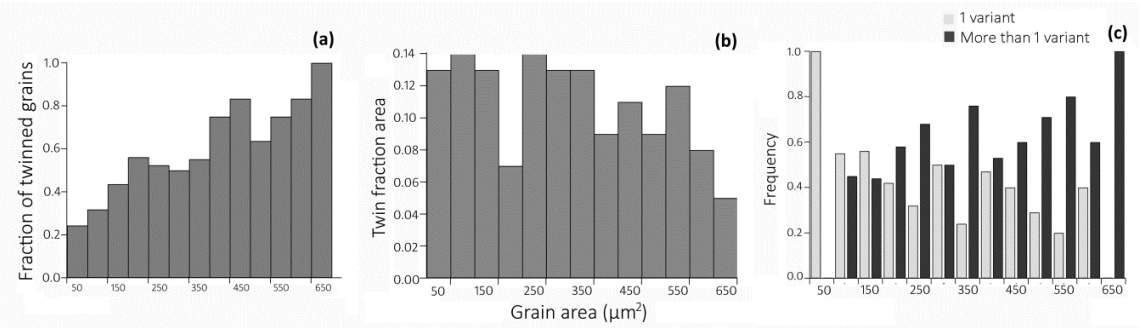

Figure 8. Effects of grain size area on (a) fraction of twinned grains, (b) twin fraction area and (c) number of variants in the grain.

The variations of fraction of twinned grains with the grain area are presented in Figure 8a. It is clearly observed that the frequency increases with the area, and that the correlation

between these parameters is strong. The trend for of the twin fraction area displays some fluctuation, but it can be concluded that the twin fraction area tends to decrease with increasing the grain area (Figure 8b). The number of variants present in one twinned grain was determined, as well (Figure 8c). The grains with small area ($\leq 50\ \mu m^2$) exhibit only one variant, while larger grains have the tendency to twin into two or more variants.

It is usually found that materials with a larger average grain size twin more easily. The effect of grain size on twinning has already been described for other hexagonal metals [4,9,10,19,29]. In those studies, three different hexagonal metals were studied: Mg and Mg alloys, Ti, and Zr. If we consider a similar grain area, up to 1000 μm^2, the correlation follows the same behavior in our present research. There is a positive correlation between the grain size and the fraction of twinned grains in all *hcp* metals. The origin of size effect on twinning is not completely understood, but some explanations have been suggested. Ecob and Ralph [30] related this effect to the concentration of dislocations in neighboring grains, while Barnett [31] considered that the number of twins is directly related to the grain boundary surface, so that a reduction of grain size will correspond to a reduced twinning.

Concerning the twin area fraction or twin volume, the results show slight discrepancies. The grain size is compared considering again the same range for grain size area, going up to 1000 μm^2. The grain area shows a strong positive influence on this parameter in titanium [4,19], the effect in magnesium is less pronounced [9,19], and is absent in zirconium [10]. For cobalt, the twin area fraction was calculated using 2D images and compared with the

grain area. In our case the twin area fraction decreases in a non-monotonous way with the grain area, which is a completely different result comparing to other *hcp* metals.

Previous studies on other hexagonal metals considered also additional parameters, as the number of twins per grain. It increases with grain size for all three metals but it is strongest for zirconium. The shape of twins in cobalt for a plastic strain of 0.04 is rather irregular, and some twins seem to be the result of twin coalescence (see in Figure 1, white arrows). In our work, we decided to estimate the number of twin variants, rather than number of twins, even if for each variant several twins can be present (see Figure 2, and 3).

At the strain level studied here, the smaller grains are less frequently twinned and present fewer twins variant. However, up to six different variants can be found for largest grain size. Concerning the presence of multiple variants (as in the present work) or multiple twins, the correlation is also positive in all hexagonal metals. The reason for such positive correlation with grain size is certainly linked to the presence of more grain boundaries being imperfect surfaces, giving nucleation sites for twinning. This is supported by atomistic simulations by Wang et al. for magnesium [32].

4. Conclusions

Polycrystalline cobalt was deformed by monotonous tensile test in the twinning work hardening stage to study the twinning deformation behavior using EBSD. The statistical analysis of twinning characteristics was performed over more than 500 grains and led to the following conclusions:

- The twin type more frequently activated is by far the $\{10\bar{1}2\}$ compression mode and this type was used for statistic considerations.
- Several variants of the $\{10\bar{1}2\}$ mode are frequently present inside a grain. The variants with higher occurrence are those with a mutual misorientation of about 60°, which correspond to the best strain accommodation inside the grain.
- Grain size seems to have less impact on twinning characteristics in comparison to orientation of grains. The twin frequency and the number of variant increase with grain size while the twin area fraction decreases.
- It is shown that the grains which are favorably oriented twin more frequently, exhibit a higher twin fraction area and several twin variants. Surprisingly, grains with their *c*-axis at 90° from the load axis are also twinned. This is probably related to a local state of stress different from the macroscopic one. These unfavorably oriented grains present lower twin area fraction and most of the time only one twin variant.

References

[1] P.G. Partridge, The crystallography and deformation modes of hexagonal close-packed metals, Metall. Rev. 12 (1967) 169–194.

[2] N. Bozzolo, L. Chan, A.D. Rollett, Misorientations induced by deformation twinning in titanium, J. Appl. Crystallogr. 43 (2010) 596–602.

[3] S. Xu, L.S. Toth, C. Schuman, J.-S. Lecomte, M.R. Barnett, Dislocation mediated variant selection for secondary twinning in compression of pure titanium, Acta Mater. 124 (2017) 59–70.

[4] M. Arul Kumar, M. Wroński, R.J. McCabe, L. Capolungo, K. Wierzbanowski, C.N. Tomé, Role of microstructure on twin nucleation and growth in HCP titanium: A statistical study, Acta Mater. 148 (2018) 123–132.

[5] J.R. Bingert, T.A. Mason, G.C. Kaschner, G.T. Gray, P.J. Maudlin, Deformation twinning in polycrystalline Zr: Insights from electron backscattered diffraction characterization, Metall. Mater. Trans. A. 33 (2002) 955–963.

[6] H. Yoshinaga, R. Horiuchi, Deformation Mechanisms in Magnesium Single Crystals Compressed in the Direction Parallel to Hexagonal Axis, Trans JIM. 4 (1963) 4–8.

[7] X.Y. Zhang, Y.T. Zhu, Q. Liu, Deformation twinning in polycrystalline Co during room temperature dynamic plastic deformation, Scr. Mater. 63 (2010) 387–390.

[8] M. Martinez, G. Fleurier, F. Chmelík, M. Knapek, B. Viguier, E. Hug, TEM analysis of the deformation microstructure of polycrystalline cobalt plastically strained in tension, Mater. Charact. 134 (2017) 76–83.

[9] I.J. Beyerlein, L. Capolungo, P.E. Marshall, R.J. McCabe, C.N. Tomé, Statistical analyses of deformation twinning in magnesium, Philos. Mag. 90 (2010) 2161–2190.

[10] L. Capolungo, P.E. Marshall, R.J. McCabe, I.J. Beyerlein, C.N. Tomé, Nucleation and growth of twins in Zr: A statistical study, Acta Mater. 57 (2009) 6047–6056.

[11] S.-G. Hong, S.H. Park, C.S. Lee, Role of {10–12} twinning characteristics in the deformation behavior of a polycrystalline magnesium alloy, Acta Mater. 58 (2010) 5873–5885.

[12] C. Guo, R. Xin, C. Ding, B. Song, Q. Liu, Understanding of variant selection and twin patterns in compressed Mg alloy sheets via combined analysis of Schmid factor and strain compatibility factor, Mater. Sci. Eng. A. 609 (2014) 92–101.

[13] M.D. Nave, M.R. Barnett, Microstructures and textures of pure magnesium deformed in plane-strain compression, Scr. Mater. 51 (2004) 881–885.

[14] X.Y. Zhang, B. Li, X.L. Wu, Y.T. Zhu, Q. Ma, Q. Liu, P.T. Wang, M.F. Horstemeyer, Twin boundaries showing very large deviations from the twinning plane, Scr. Mater. 67 (2012) 862–865.

[15] Q. Sun, X.Y. Zhang, R.S. Yin, Y. Ren, L. Tan, Structural characterization of {1013} twin boundaries in deformed cobalt, Scr. Mater. 108 (2015) 109–112.

[16] Q. Sun, X.Y. Zhang, Y.C. Wang, Y. Ren, L. Tan, Q. Liu, Structural characterization of twin boundaries in deformed cobalt, Mater. Charact. 116 (2016) 44–47. doi:10.1016/j.matchar.2016.04.005.

[17] G. Fleurier, E. Hug, M. Martinez, P.-A. Dubos, C. Keller, Size effects and Hall–Petch relation in polycrystalline cobalt, Philos. Mag. Lett. 95 (2015) 122–130.

[18] Y.. Wang, J.. Huang, Texture analysis in hexagonal materials, Mater. Chem. Phys. 81 (2003) 11–26.

[19] A. Ghaderi, M.R. Barnett, Sensitivity of deformation twinning to grain size in titanium and magnesium, Acta Mater. 59 (2011) 7824–7839.

[20] N. Dixit, K.Y. Xie, K.J. Hemker, K.T. Ramesh, Microstructural evolution of pure magnesium under high strain rate loading, Acta Mater. 87 (2015) 56–67.

[21] Y. Pei, A. Godfrey, J. Jiang, Y.B. Zhang, W. Liu, Q. Liu, Extension twin variant selection during uniaxial compression of a magnesium alloy, Mater. Sci. Eng. A. 550 (2012) 138–145.

[22] A. Ostapovets, P. Molnár, On the relationship between the “shuffling-dominated” and “shear-dominated” mechanisms for twinning in magnesium, Scr. Mater. 69 (2013) 287–290. doi:10.1016/j.scriptamat.2013.04.019.

[23] J.J. Jonas, S. Mu, T. Al-Samman, G. Gottstein, L. Jiang, Ė. Martin, The role of strain accommodation during the variant selection of primary twins in magnesium, Acta Mater. 59 (2011) 2046–2056.

[24] S. Mu, J.J. Jonas, G. Gottstein, Variant selection of primary, secondary and tertiary twins in a deformed Mg alloy, Acta Mater. 60 (2012) 2043–2053.

[25] D. Ando, J. Koike, Y. Sutou, Relationship between deformation twinning and surface step formation in AZ31 magnesium alloys, Acta Mater. 58 (2010) 4316–4324.

[26] Y.T. Zhu, X.Y. Zhang, Q. Liu, Observation of twins in polycrystalline cobalt containing face-center-cubic and hexagonal-close-packed phases, Mater. Sci. Eng. A. 528 (2011) 8145–8149.

[27] C. Lou, X. Zhang, Y. Ren, Non-Schmid-based {10-12} twinning behavior in polycrystalline magnesium alloy, Mater. Charact. 107 (2015) 249–254.

[28] F. Xu, X. Zhang, H. Ni, Y. Cheng, Y. Zhu, Q. Liu, Effect of twinning on microstructure and texture evolutions of pure Ti during dynamic plastic deformation, Mater. Sci. Eng. A. 564 (2013) 22–33. doi:10.1016/j.msea.2012.11.097.

[29] M.R. Barnett, Z. Keshavarz, A.G. Beer, D. Atwell, Influence of grain size on the compressive deformation of wrought Mg–3Al–1Zn, Acta Mater. 52 (2004) 5093–5103.

[30] N. Ecob, B. Ralph, The effect of grain size on deformation twinning in a tectured zinc alloy, 18 (1983) 2419–2429.

[31] M.R. Barnett, Z. Keshavarz, A.G. Beer, X. Ma, Non-Schmid behaviour during secondary twinning in a polycrystalline magnesium alloy, Acta Mater. 56 (2008) 5–15.

[32] J. Wang, I.J. Beyerlein, C.N. Tomé, An atomic and probabilistic perspective on twin nucleation in Mg, Scr. Mater. 63 (2010) 741–746.